J. Phys. Chem. A **1999,** *103,* 8927−8934

Assignment of the $\tilde{B}^+$ State of the Chlorobenzene Cation Using Photoinduced Rydberg Ionization (PIRI) Spectroscopy

R. Anand, J. D. Hofstein,[†] J. E. LeClaire, and P. M. Johnson*

Department of Chemistry, The State University of New York at Stony Brook,
Stony Brook, New York 11794-3400

C. Cossart-Magos

Laboratoire de Photophysique Moléculaire du CNRS, Institut de Physico-Chimie Moléculaire,
Bâtiment 213, Université de Paris-Sud, F-91405 Orsay Cedex, France

Received: July 1, 1999; In Final Form: September 3, 1999

The photoinduced Rydberg ionization (PIRI) spectra of the $\tilde{B}^+$ state of the chlorobenzene cation were recorded via the origin, 6b, and 16a16b vibrations of the cation ground state ($\tilde{X}^+$). The resonance-enhanced multi photon dissociation spectroscopy (REMPD) spectrum of the $\tilde{B}^+ \leftarrow \tilde{X}^+$ transition of the chlorobenzene cation was also obtained. To date it has been thought that $\tilde{B}^+ \leftarrow \tilde{X}^+$ is an electronically forbidden transition (C_{2v} symmetry), taking place from the $^2B_1$ ground state to a $^2B_2$ excited state. The ability of PIRI to provide spectra from specific lower-state vibrational levels allowed this hypothesis to be tested, because the 16a vibration would be the primary inducing mode in the transition. Assuming a forbidden transition, a comparison between the spectrum from the ground-state origin and that from the 16a16b vibration would necessitate an assignment that gives unlikely vibrational frequencies. It is therefore concluded that the $\tilde{B}^+ \leftarrow \tilde{X}^+$ transition of chlorobenzene is electronically allowed. Configuration interaction of singles (CIS) and complete active space multiconfigurational self-consistent field (CASSCF) calculations with 6-31G** basis sets were performed to ascertain the symmetry assignments of the excited ionic states. These calculations resulted in the possibility that at least one excited state of the cation of $^2B_1$ symmetry lies below any state of $^2B_2$ symmetry. Hence, we propose that the ionic transition observed in the acquired PIRI/REMPD spectra of the cation is an allowed transition to a $^2B_1$ state, thus giving rise to the observation of the origin of the $\tilde{B}^+$ state at 18 219 cm^{-1}.

Introduction

Much of the understanding of the reactivities and chemical properties of molecules is based on a fundamental knowledge of the molecular orbital ordering and the geometric structure. This understanding of molecular properties is directly affected by the assignment of cationic excited states. However, in the past, relatively low-resolution experimental techniques have prevented an unambiguous analysis of many excited ionic states. The development and utilization of laser techniques and the use of Rydberg states has improved the resolution achievable in cationic spectroscopic studies so that it is on the order of the laser bandwidth, which provides capabilities for improved assignments.

A newly developed spectroscopic technique in our laboratory, called photoinduced Rydberg ionization (PIRI)[1] spectroscopy, has been successfully applied to vibrationally resolved studies of the electronic excited states of various molecular ions. The $\tilde{B}^+$ state of the benzene cation,[2] as well as substituted benzene cations, phenol,[3] and fluorobenzene,[4] have been described in detail previously. Basically, the PIRI technique utilizes the long-lived Rydberg series converging onto the ground ionic state as intermediate states to access the excited electronic states of the cation. Because the Rydberg electron interacts very little with optical radiation or the core orbitals, the absorption cross sections for a Rydberg molecule, in the visible as well as ultraviolet (UV) region, correspond almost exactly to that of the bare ion.

The PIRI technique is built on mass-analyzed threshold ionization (MATI)[5] spectroscopy. In PIRI, first the Rydberg molecules are created by a two-color, two-photon excitation, and prompt ions are spatially separated from the neutral Rydberg molecules as in MATI. Then, a third tunable laser beam (PIRI laser) is sent coaxially down the molecular beam to irradiate the Rydberg molecules and to create core-excited Rydberg molecules. When the PIRI laser is tuned to a cationic transition, it causes rapid autoionization. The group of ions formed from autoionization (parent PIRI ions) are spatially separated from the remaining Rydbergs and then detected in a time-of-flight mass spectrometer (TOFMS). The high-resolution spectrum of the electronically excited cationic state is obtained by scanning the third PIRI laser, which basically simulates the spectrum of the ion core. Alternatively, the PIRI light can be focused to create a resonant multiphoton transition of the core, dissociating the cation and simultaneously causing autoionization. Fragment ions are then detected in mass channels free from any background interference caused by spontaneous autoionization (called fragment PIRI).[3]

---

* Author to whom correspondence should be addressed. E-mail: *pJohnson@sunysb.edu.*

[†] Present address: American Physical Society, Ridge, New York 11961.

10.1021/jp992263p CCC: $18.00

Here we report the application of the PIRI technique to a study of the $\tilde{B}^+$ state of the chlorobenzene cation. This ion has received much attention to study the effects of the substitution of a heavy halogen atom on the benzene ring.[6] Various photoelectron spectroscopy (PES) studies on different substituted benzene molecules have been carried out, exploring the effects of substitution on the benzene ring and assigning the symmetries and the energies to the states.[7] Numerous low-resolution studies such as Penning ionization electron spectroscopy (PIES),[8] and emission spectroscopy[9] have also been performed to elucidate the energies and the symmetries of chlorobenzene cation states. In all, these experiments have inferred that the symmetry of the $\tilde{B}^+$ state is $^2B_2$, though the proximity of the $\tilde{C}^+$ state to the $\tilde{B}^+$ state makes the assignment somewhat difficult. Fluorescence emission studies[10] on the chlorobenzene cation and the calculations done so far suggest that the $\tilde{B}^+$ state of the cation has a half-filled σ orbital (a σ-state). This suggestion is inferred because the fluorescence quantum yields of emission are very small (of the order of $\leq 10^{-5}$), similar to benzene where fluorescence is also not observed and the $\tilde{B}^+$ state is known to have σ character. It is the purpose of this paper to use the high resolution and selective vibrational excitation of PIRI, along with electronic structure calculations, to examine the validity of the accepted $^2B_2$ assignment of the $\tilde{B}^+$ state of chlorobenzene.

High-resolution multiphoton ionization−photoelectron spectroscopy (MPI−PES),[11] zero-electron kinetic energy−pulsed field ionization (ZEKE−PFI)[12] spectroscopy, and MATI[13] studies exist for the chlorobenzene in the ground ionic state [ionization potential (IP_0) = 73 170 cm^{-1}]. By these methods, various vibrational frequencies have been well defined in the ground ionic state. Resonance-enhanced mulitiphoton dissociation spectroscopy (REMPDS) technique, developed initially by Woodward et al. to study *trans*-1, 3-butadiene,[14] has been successfully applied to study some excited ionic states of benzene[15] and substituted benzenes, including chlorobenzene cation.[16] The PIRI and REMPDS techniques give similar information, though there lies a subtle difference in the two methods that is useful in the complete analysis of the excited state of any cation.

REMPDS can provide high-resolution spectra of the excited states of cations and give valuable insights into their electronic and vibrational character. In the REMPDS technique, a laser prepares a sample of ions by resonant two-photon absorption from the neutral ground state. This sample of ions is then excited by a second tunable laser that causes resonant multiphoton transitions in the cations, resulting in dissociation. The presence of fragment ions indicates a cationic resonance, and thus an electronic spectrum of the ion is attained as the laser is scanned to appropriate wavelengths. In REMPDS, the multiphoton nature of the ion excitation results in some line broadening, and the process of ion creation leaves them in vibrationally excited states, resulting in a congested spectra. In the PIRI technique however, using Rydbergs appearing in close proximity of the ion state results in a high-resolution spectrum originating from a given specified vibrational level, devoid of hot-band structure. If the Rydbergs are not separated from prompt ions in a fragment PIRI experiment, a REMPD spectrum results.

The most useful previous spectrum of the chlorobenzene cation for the $\tilde{B}^+ \leftarrow \tilde{X}^+$ transition is a REMPD spectrum taken by Ripoche et al.[16] Their assignment of the $\tilde{B}^+$ state as $^2B_2$ is mainly based on the matrix absorption spectra of the chlorobenzene cation,[17] where it can be argued that the weak transitions observed between 540 and 490 nm are due to an electronically forbidden $\tilde{B}^+ \leftarrow \tilde{X}^+$ transition. Accepting the $^2B_2$ assignment, they proposed 16a and 10a modes of a_2 symmetry appear as strongly inducing bands with progressions of mainly symmetric vibrations built on them. An interesting feature of their vibrational analysis is that the 16a mode appears in the great majority of their assignments. Subtracting this mode from each of the assignments would make the analysis consistent with an allowed rather than a forbidden transition.

Electronic structure calculations performed in past have primarily been on neutral chlorobenzene, the most recent being that performed by Fujisawa et al.,[8] and the assignments of the excited ionic states have been based on the validity of Koopmans' theorem.[7] However, the ground ionic spectrum of the cation has been well categorized.[12,13] Because of this good categorization and because the REMPD spectrum includes considerable hot-band structure that makes analysis difficult, it was desirable to obtain a cold PIRI spectrum of the chlorobenzene cation via the origin and the nonsymmetric vibrations of the ground ionic state ($\tilde{X}^+$ state). In addition, electronic structure calculations were also performed to provide clues as to the nature of the $\tilde{B}^+$ state. The results of the PIRI spectra, combined with ab initio calculations performed for the ionic states, indicate that an excited state of $^2B_1$ symmetry lies lower than any $^2B_2$ state and is the probable terminus of the $\tilde{B}^+ \leftarrow \tilde{X}^+$ transition, which is now electronically allowed.

Experimental Section

The apparatus used to obtain the PIRI spectra of the chlorobenzene cation is similar to that used for substituted benzene experiments and has been described in detail previously.[3,4] It basically consisted of two differentially pumped vacuum chambers within which the supersonic molecular beam of the sample was created by a variable-temperature-pulsed nozzle in the sample chamber. The molecular beam for chlorobenzene was created by heating a sample cell containing chlorobenzene seeded with He gas with the backing pressure of ∼2.7 atm, and skimming the sample prior to its entrance into the ionization chamber. Both the sample container and the pulsed nozzle were heated to temperatures between 65 and 70 °C. The ionization chamber contained a Wiley−McLaren type, TOFMS detection system. Typical source chamber pressure was in the 1×10^{-5} Torr range, and that of the ionization region was between 7×10^{-7} and 2×10^{-6} Torr.

Coumarin 522B dye was used in a Quanta-Ray PDL1 dye laser to resonantly excite the molecule to its S_1 state. Rhodamine 575 dye in a Lambda-Physik FL2002 dye laser was then used to create Rydbergs converging on the origin and the excited vibrational states in the ground state of the cation. Both of these dye lasers were pumped with the same Nd:YAG laser. To acquire the PIRI spectra of the $\tilde{B}^+$ state of the cation, various dye outputs in the wavelength range covering ∼510−565 nm were used in a Lumonics HyperDYE-300 laser pumped by 355 nm light from a second Nd:YAG laser. To record the REMPD spectrum of the chlorobenzene cation, Coumarin 522B dye in a Quantel TDL50 dye laser was used to access the S_1 state and Fluorescein 548 dye was then used to access the ground ionic state of the cation. Both the dye lasers were pumped by a Nd:YAG laser. The REMPD spectra were taken in the energy range 490−566 nm. The third tunable photon was provided by a second Nd:YAG laser pumping a single dye laser, Quantel TDL50. Typically, the frequency-doubled output power for both Rydberg preparation lasers was 0.5−1.5 mJ per laser shot. The visible output power obtained from the third PIRI/REMPD laser was typically 8−10 mJ per laser shot. The parent PIRI spectrum was acquired by gently focusing the PIRI light down the

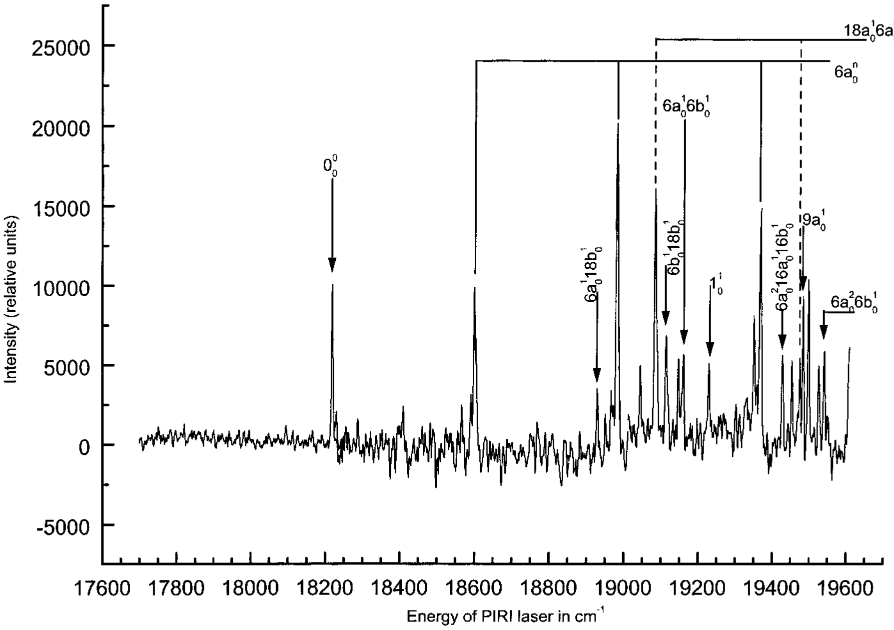

Figure 1. Vibrationally resolved parent PIRI spectrum of the $\tilde{B}^+$ state of the chlorobenzene cation via the origin of the ground electronic state. The *x*-axis is the excess energy (cm^{-1}) of the PIRI laser above the ground ionic state.

molecular beam to avoid any fragmentation of the prepared Rydbergs in the ground ionic state. The acquisition of the fragment PIRI spectra was facilitated by tighter focus of the PIRI light down the molecular beam. For each dye, the laser used to obtain the PIRI spectra was calibrated against neon absorption lines to within an error of 1 cm^{-1}.[3] In the case of chlorobenzene, because the lifetime of the S_1 state is <1 ns, it was necessary to overlap the Rydberg preparation lasers temporally at the sample. The voltage separation scheme used in the PIRI technique to separate the three packets of ions in the ionization region and their detection has been described in detail previously.[4]

Electronic structure calculations, including geometry optimization, population analyses, and normal mode calculations, were all done using GAUSSIAN 94[18] and Gamess.[19] Density functional theory (B3LYP) calculations were done using a 6-31G** basis set both on the ground state ($^2B_1$) and the first excited σ state ($^2B_2$) of the chlorobenzene cation, keeping the ion in C_{2v} symmetry. As usual for this type of calculation, it was not possible to examine any excited state of the same symmetry as the ground ionic state using Hartree−Fock methods alone. To determine state ordering, configuration interaction of singles (CIS), configuration interaction of singles, doubles, and triples (CISDT), and complete active space multiconfigurational self-consistent field (CASSCF) methods were employed. The vibrational modes calculated for the chlorobenzene cation can be numbered simply by comparing the atomic motions to those of vibrations calculated for a benzene ring. However, some vibrational modes in the chlorobenzene cation do not have corresponding parent ring vibrations because of the heavy chlorine atom substitution on the benzene ring. When the numbering is ambiguous while considering only the atomic motions, the vibrational features have been numbered simply by comparing their motions and frequency values to established vibrational assignments for the neutral chlorobenzene.

Results and Discussion

The parent PIRI spectrum of the $\tilde{B}^+$ state was recorded via the origin of the ground electronic state ($\tilde{X}^+$ state) of the chlorobenzene cation, as shown in Figure 1, and fragment PIRI spectra were recorded via the nonsymmetric vibrations 6b and 16a16b of the ground ionic state, as shown in Figure 2. For reference, a REMPD spectrum taken during this study is shown in Figure 3. This spectrum is similar to that of Ripoche et al.[16] The REMPD spectrum was produced both by the absorption of multiple photons of λ_1 (used to make a transition from S_0 state to S_1 state) and the Rydbergs created by the second photon (λ_2 photon used to make the S_1 to $\tilde{X}^+$ transition), which were not separated from the prompt ions. The ions could thus have as much as 925 ± 5 cm^{-1} of energy at their creation ($2\lambda_1 = 74\,104$ cm^{-1}).

In the PIRI spectra of the chlorobenzene cation via the origin, and 16a16b and 6b vibrations of the cationic ground state, one main intense vibrational progression is observed along with dense vibrational features at higher energy. The vibrational structure observed is similar to that seen in the PIRI spectra of the fluorobenzene cation.[4] The progressions are not as extensive and anharmonic as were observed in the case of the PIRI spectra of the phenol cation obtained in our laboratory previously,[3] and therefore indicate no major geometry change (unlike phenol) for the chlorobenzene cation. The widths of the peaks are ∼3−5 cm^{-1}, and the peaks neither become broad nor does the intensity increase as one goes higher in energy. However, an interesting feature exists in this cold PIRI spectrum; that is, the vibrational structure at low energy is very sparse compared with the more congested vibrational features at higher energy and in the REMPD spectrum.

The PIRI spectrum obtained for the $\tilde{B}^+$ state provides new information about the chlorobenzene cation in the excited ionic state because hot bands are eliminated. If a $^2B_2$ assignment of the $\tilde{B}^+$ state were correct, then the first peak should be the $16a^1_0$ false origin, with totally symmetric vibrations built on it and also on the other a_2-inducing modes, $10a^1_0$ and $17a^1_0$. In the PIRI spectrum via the origin of the $\tilde{X}^+$ state, we observe a main intense 6a progression at an energy spacing of ∼384 cm^{-1}, but nothing else appears until almost 700 cm^{-1}. The PIRI spectrum does not show pure $10a^1_0$ or $17a^1_0$ transitions, which logically should appear in the gap between the second peak and the remaining dense structure if the $\tilde{B}^+ \leftarrow \tilde{X}^+$ were an electronically forbidden transition (see Figure 1). The peaks assigned to $10a^1_0$

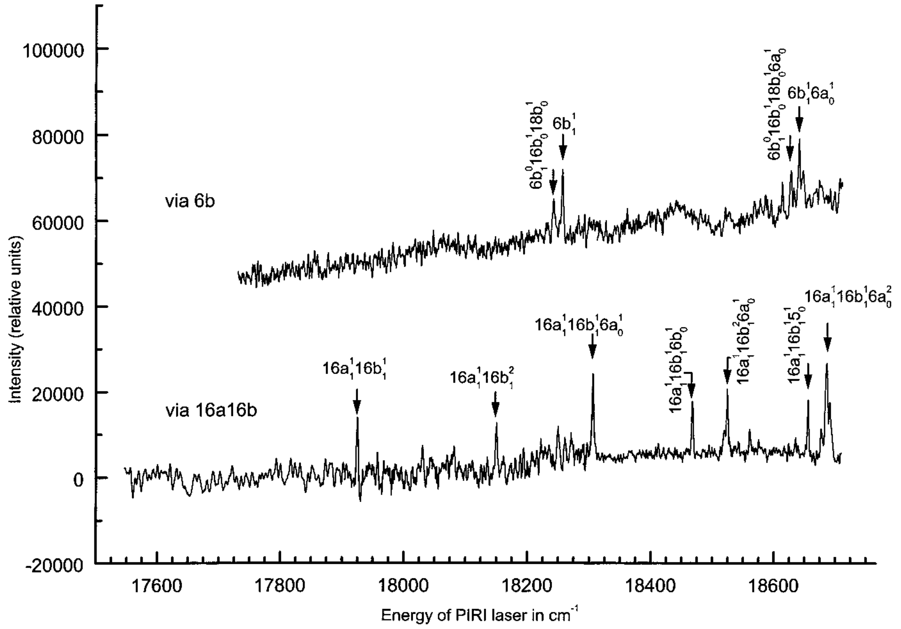

Figure 2. The fragment PIRI spectra of the $\tilde{B}^+$ state of the chlorobenzene cation via the 16a16b and 6b vibrational levels of the ground state. The *x*-axis denotes the energy of the PIRI laser (cm^{-1}) above the ground ionic state.

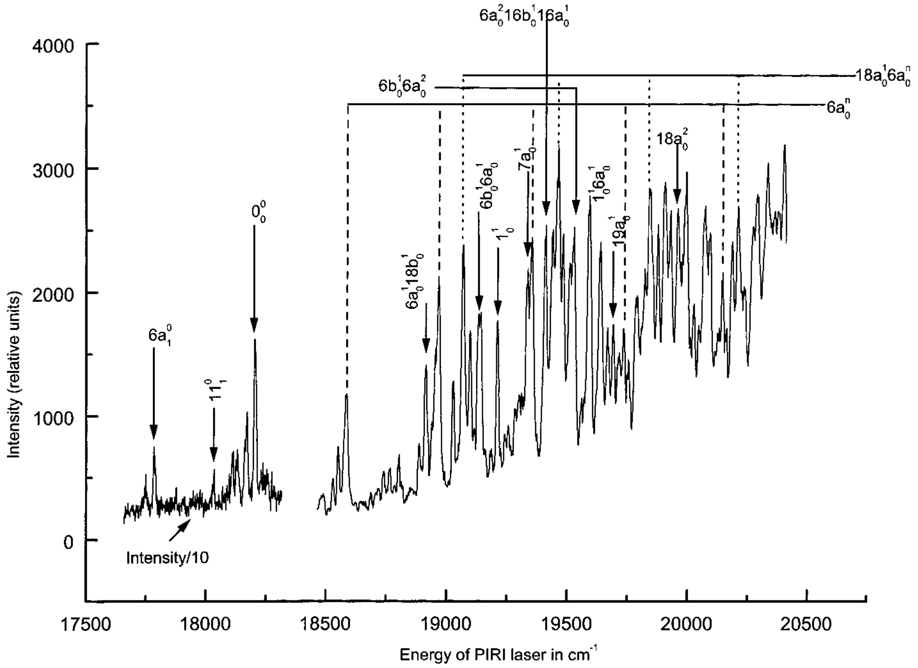

Figure 3. The REMPD spectrum of the $\tilde{B}^+$ state of the chlorobenzene cation recorded during this study. The *x*-axis is the excess energy of the third laser above the ground ionic state.

and $6a^1_0 10a^1_0$ by Ripoche et al.[16] in the REMPD spectrum do not appear in the PIRI spectrum and are apparently hot bands.

The PIRI spectra of the $\tilde{B}^+$ state of the chlorobenzene cation were also obtained via the excited vibrational levels of the ground state, 16a16b and 6b (both of b_2 symmetry) to confirm the symmetry assignment of the $\tilde{B}^+$ state (see Figure 2). Most of the vibrational features observed in the spectra again can be assigned for either an allowed or a forbidden electronic transition. If $\tilde{B}^+ \leftarrow \tilde{X}^+$ were a forbidden transition, the origin of the $\tilde{B}^+$ state could in principle be observable from the b_2 vibrational states of the ground ionic state. No such structure was observed at the required energy value in the PIRI spectra via either the 16a16b (b_2) or 6b(b_2) vibrations of the ground ionic state (see Figure 2), but this could either be attributed to the transition being allowed or to the lines being weak because of small transition moments for this vibronic symmetry.

Strong evidence that the $\tilde{B}^+ \leftarrow \tilde{X}^+$ transition is allowed comes by comparing the vibrational features observed in the PIRI spectra acquired via the origin and the 16a16b vibrations of the ground ionic state. If the $\tilde{B}^+$ state were of $^2B_2$ symmetry, the only logical way to assign the PIRI spectrum acquired via the 16a16b vibration of the ground cationic state would be to assign the first peak observed at 17 924 cm^{-1} as the $16a^0{}_1 16b^1{}_1$ transition, because an a_2-inducing vibration should be gained or lost in any transition (Figure 2). Moreover, for a forbidden electronic transition via the origin of the $\tilde{X}^+$ state, the first vibrational line observed in the PIRI spectrum (Figure 1) at 18 219 cm^{-1} would be the $16a^1{}_0$ vibration (a_2 symmetry). From

TABLE 1: Experimental and Theoretical Vibrational Frequency Values for Various States of Chlorobenzene[a]

	calculated values[b]			experimental values				
vibrational states	$\tilde{X}^+$ ($^2B_1$) B3LYP/6-31G**	$\tilde{B}^+$ ($^2B_2$) B3LYP/6-31G**	S_0[c]	S_1[d]	$\tilde{X}^{+d}$	$\tilde{X}^+$ ZEKE[e]	$\tilde{X}^+$ MATI[c]	$\tilde{B}^+$ ($^2B_1$) (allowed)
1(a_1)	991	988	1003	931	981	975	971	1010
6a(a_1)	425	377	417	378	421	422	420	384
7a(a_1)	1119	1122	1093	1065	1106	1116	1115	1131
9a(a_1)	1220	1445	1153	981	1182	1200	1194	1263
12(a_1)	720	606	707	671	728	716	714	636
18a(a_1)	1003	839	1026	966	1016	995	992	866
19a(a_1)	1466		1482[e]			1429		1488
10a(a_2)	804	806	831[e]			808(calc)		
16a(a_2)	359	256	403	203	342	348	343	223
17a(a_2)	1009	560	962[e]			1010(calc)		
4(b_1)			684[e]	422[d]	558			
5(b_1)			981[e]	699[d]	909			730
10b(b_1)	1022	1003	741[e]	556[d]	603			
11(b_1)	150	179	197[e]	138[d]	165	144(calc)		
16b(b_1)	404	445	467	320	388	394	393	218
17b(b_1)		899	903[e]	655[d]	812	960(calc)		
6b(b_2)	534	514	615	521	526	531	526	562
18b(b_2)	306	191	295	287	322	311		329
16a16b(b_2)		701		524			736	441

[a] Observed frequencies are included for the S_0 and S_1 states of the neutral and for the ground and the excited ionic state with $^2B_1$ symmetry (from the PIRI spectra of the cation) of the cation. Calculated vibrational values are presented for the ground state ($\tilde{X}^+$ state) and the σ state of $^2B_2$ symmetry for the cation. [b] The calculated frequency values for the $\tilde{X}^+$ state ($^2B_1$) and the $\tilde{B}^+$ state ($^2B_2$) have been corrected with an optimal scaling factor (0.9613 for B3LYP/6-31G**) [c] See ref 13 and references within. [d] See ref 11c. [e] See ref 12.

the absolute positions of these two lines, plus the known frequency of the 16a16b vibration in the ground state, the energy difference between the 16a and16b vibrations in a hypothetical $\tilde{B}^+$ ($^2B_2$) state is easily determined to be 441 cm^{-1}. This result is highly unlikely when compared with the energy difference of 46 cm^{-1} in the ground ionic state,[11,12,13] and compared with calculated frequencies for a $^2B_2$ state. The value for the 16a vibration in a $^2B_2$ state could be estimated by assuming the peak observed at 18 467 cm^{-1} to be $16a^2{}_1 16b^1{}_1$. Ignoring anharmonicity, this assumption gives an approximate value of 16a of 272 cm^{-1}, which is close to the calculated value of 256 cm^{-1} (see Table 1). This assignment, therefore results in the 16b vibration being 713 cm^{-1} in the excited $\tilde{B}^+$ state. Such a major increase in the frequency of the 16b vibration in the excited state from that of the ground ionic state (394 cm^{-1})[12,13] also stretches the bounds of credibility. Other assignments for the $16a^2{}_1 16b^1{}_1$ transition in the PIRI spectrum via the 16a16b vibration for a nonallowed transition would result in even higher values of 16b in the $\tilde{B}^+$ state. Thus, on the basis of the these contradictions, it is strongly indicated that $\tilde{B}^+ \leftarrow \tilde{X}^+$ is an allowed π to π transition.

If further evidence is needed, we can look to the REMPD spectrum for another feature that should be prominent in a transition to a $^2B_2$ state; that is, a $16a^0{}_1$ hot band. A hot band $16a^0{}_1$ vibrational mode is not observed in the spectrum even though the position of this line is predictable based on the fact that the ground-state vibrations are well known. It has been argued[16] that the $16a^0{}_1$ transition is missing because 16a is not populated upon creating the ion from the S_1 state. However, 16a appears in the ZEKE spectrum of Wright et al.[12] as well as Lembach's MATI spectrum,[13] so it clearly has some oscillator strength in the ionization process. In addition, the copious amount of hot-band structure in the REMPD spectrum is evidence that a great amount of intramolecular vibrational relaxation (IVR) is taking place, which would populate such a low-lying vibrational level as 16a. Our vibrational assignment of the REMPD hot-band structure, as well as Ripoche's, would not make sense without the existence of IVR.

Finally, a less compelling indication that a $^2B_2$ assignment may be wrong for the $\tilde{B}^+$ state is the frequency of the 16a vibration. From the REMPD spectra,[16] the energy of the 16a vibrational mode had been tentatively assigned as 179 cm^{-1} on the basis of the suggested appearance of odd vibrational modes, $16a^3$ and $16a$,[5] positioning the origin of the $\tilde{B}^+$ state at 18 034 cm^{-1}. From density functional (B3LYP) calculations using a 6-31G** basis set on the excited ionic state ($^2B_2$ symmetry), the frequency of 16a was found to be 256 cm^{-1}, which is much different from the value (179 cm^{-1}) previously proposed. Normal mode calculations were also performed on the ground state of the cation, and the frequency values obtained were found to agree very well with the experimental ground-state values (e.g., see the paper by Wright et al.[12] and references within). The calculated frequency values, along with their respective symmetries of the ground ionic state in $^2B_1$ symmetry and the excited ionic state in $^2B_2$ symmetry, are given in Table 1 along with the values obtained by Asselin et al.,[11] Wright et al.,[12] and Lembach et al.[13]

To determine the probable symmetry of the $\tilde{B}^+$ state, electronic structure calculations were performed to ascertain the ordering and symmetries of the first few excited ionic states. CIS calculations using Gaussian 94 on chlorobenzene cation for the ground and the first four excited ionic states (at the ground-state geometry) revealed an energy ordering of $^2B_1$, $^2A_2$, $^2B_1$, $^2B_2$, and $^2B_1$, starting at the ground state, though the energy values (in Table 2) are much higher than the experimental values obtained.[7] This result suggests that one of the excited ionic states of $^2B_1$ symmetry is lower in energy than the lowest state with $^2B_2$ symmetry. Apparently because of the proximity of several states, we were not able to get CIS geometries to optimize for excited states. Therefore, the only excited-state vibrational frequencies obtained were with density functional theory (DFT) for the $^2B_2$ state.

Configuration interaction (CI) was also performed using Gamess,[19] using various combinations of virtual and occupied core orbitals in the active space. Depending on the number of valence and occupied orbitals in the active space, it was found that the stabilization of the σ and the π orbitals varied with respect to each other. At the largest CI we could perform (which included singles, doubles, and triples from all of the valence orbitals into 10 virtual orbitals) it was found that the second

TABLE 2: Excited-State Energies of the Chlorobenzene Cation Obtained from the CIS/6-31G using Gaussian 94 and CI/6-31G using Gamess, Along with the Symmetry of the States and the Experimentally Acquired Values from PES[7] [a]**

states	energy values obtained from CIS/6-31G** using Gaussian 94, eV	energy values obtained from CI/6-31G using Gamess, eV	experimental values from PES,[7] eV
$\tilde{A}$	$1.28/^2A_2$	$1.14/^2A_2$	$0.57/^2A_2$
$\tilde{B}$	$3.11/^2B_1$	$3.36/^2B_2$	$2.24/^2B_2$
$\tilde{C}$	$4.46/^2B_2$	$3.38/^2B_1$	$2.6/^2B_1$
	$4.67/^2B_1$	$4.57/^2B_2$	$3.19/^2A_1$

[a] The symmetry of the ground ionic state ($\tilde{X}^+$ state) is $^2B_1$. The energy value obtained from CASSCF calculations for the second excited state ($^2B_1$ symmetry) is 3.49 eV. Calculations were not done for states of $^2A_1$ symmetry. The experimental value of the $\tilde{B}^+$ state ($^2B_1$ symmetry) is 2.26 eV.

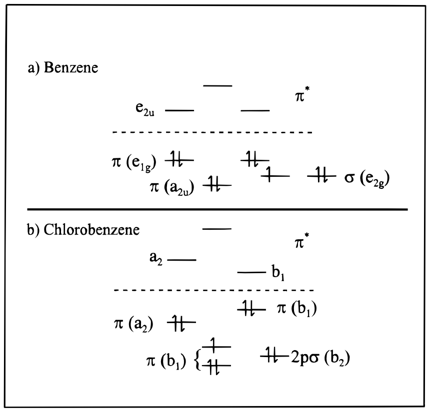

Figure 4. Molecular energy level diagram for (a) benzene, (b) chlorobenzene ionic species including π, π^*, and the highest occupied σ orbitals along with their symmetries. For CASSCF calculations on chlorobenzene cation, 1 b_2 and 4 b_1 orbitals and 7 electrons were included in the active space as shown.

and the third excited ionic states are very close in energy, so as to be basically degenerate.

To further corroborate the results obtained from CIS calculations, CASSCF calculations were performed with a 6-31G** basis set. The valence orbitals and electrons that were taken into account are shown in Figure 4. The active space was specified to incorporate the four π orbitals of b_1 symmetry and one σ orbital of b_2 symmetry, thus including 7 electrons and 5 orbitals in the active space. The geometry optimization of the first excited root gave the symmetry of the state as $^2B_1$ symmetry, which is actually the second excited state of the ion because a_2 orbitals were not included in the active space. Calculations for the higher roots failed to converge and thus their energies could not be determined at an optimized geometry. In these calculations, 4 orbitals of b_1 symmetry and only 1 ortibal of b_2 symmetry were taken into account, so there was much more configuration interaction in the π manifold. However, because other b_2 orbitals are somewhat distant in energy from the one considered, these results give another indication that there is a $^2B_1$ excited state below the first $^2B_2$ state. A point to note is that in the calculations performed, we have directly calculated the energy and geometry optimizations of the ionic states, unlike previous calculations in which the ionic state energies were derived from the orbital energies obtained in calculations on the neutral molecule.

The identity of the half-filled orbital for the lowest excited $^2B_1$ state can be obtained from the population analyses in both the DFT and CIS calculations. These calculations show that substitution of a chlorine atom onto the benzene ring creates an interaction of the lower π orbital of benzene (a_{2u} symmetry in benzene) with the $3p_z$ orbital of chlorine, giving rise to two b_1 orbitals, as shown in Figure 4. The splitting caused by this interaction apparently moves the upper member of this pair above the b_2 σ orbital and changes the normal ordering of the states, as was seen in fluorobenzene.[4] The resulting bonding and the antibonding orbitals of b_1 symmetry show that the electron densities are evenly spread over both the chlorine atom and the benzene ring, as shown in Figure 5. This situation is unlike the case of flourobenzene[4] where the electron densities were concentrated either on the ring or the fluorine in the individual bonding and antibonding orbitals.

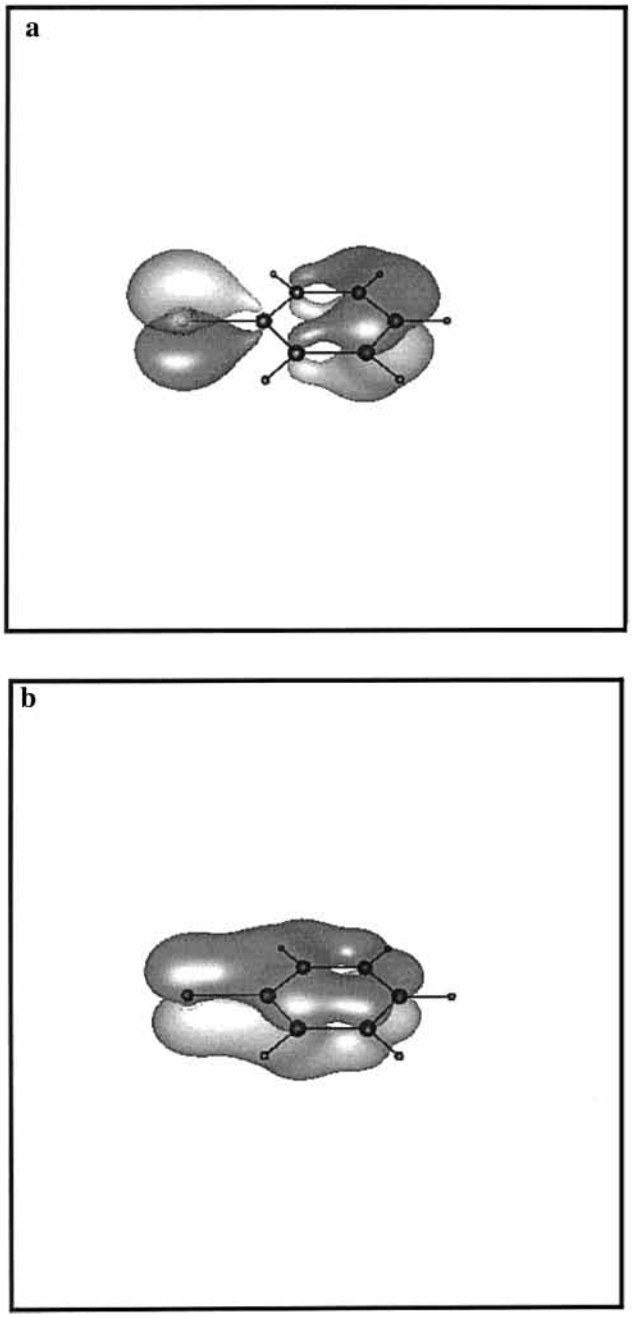

Figure 5. The electron density distributions of the orbitals of b_1 symmetry resulting from the interaction of the $3p_z$ chlorine orbital with the lowest π ring orbital of a_{2u} symmetry, obtained from Hartree–Fock method. The electron density distributions, unlike for fluorobenzene cation,[4] are evenly distributed between the chlorine atom and the benzene ring. (a) $\pi(b_1)$. (b) $\pi(\beta_1)$.

TABLE 3: Energy of the PIRI Laser and the Proposed Assignments of the Vibrational Features Observed in the PIRI Spectrum via the Origin of the $\tilde{X}^+$ State of the Chlorobenzene Cation for the $\tilde{B}^+(^2B_1)\leftarrow\tilde{X}^+(^2B_1)$ Transition

frequency (cm^{-1})	proposed assignment	distance from origin (cm^{-1})
18 219	0^0_0	0
18 599	$6a^1_0$	381
18 929	$6a^1_0 18b^1_0$	710
18 980	$6a^2_0$	761
19 044	$6a^1_0 16a^1_0 16b^1_0$	825
19 084	$18a^1_0$	865
19 114	$6b^1_0 18b^1_0$	895
19 146		927
19 162	$6a^1_0 6b^1_0$	942
19 229	1^1_0	1010
19 349	$7a^1_0$	1130
19 367	$6a^3_0$	1148
19 428	$6a^2_0 16a^1_0 6b^1_0$	1209
19 451		1232
19 476	$18a^1_0 6a^1_0$	1257
19 483	$9a^1_0$	1264
19 497	$6b^1_0 18b^1_0 6a^1_0$	1278
19 525		1306
19 541	$6b^1_0 6a^2_0$	1322

The PIRI spectra of the $\tilde{B}^+$ state via the 16a16b vibration has been assigned assuming it is an allowed transition, with the peak at 17 924 cm^{-1} as $16a^1_1 16b^1_1$ and symmetric vibrational progression built upon it. This assignment leads to a decrease of 295 cm^{-1} in the value of the16a16b combination in the excited state. The frequency values of the 16a and the 16b vibrations in the excited cationic state also decrease considerably from the $\tilde{X}^+$ state, to 223 and 218 cm^{-1} respectively. These values are comparable to the values in the S_1 state of neutral chlorobenzene[11,12] (refer to Table 1). This decrease in the 16a and 16b values from the ground ionic state to the excited state could be because removal of the electron takes place from the most strongly bonding π orbital of the ring in the $\tilde{B}^+\leftarrow\tilde{X}^+$ transition, (see Figure 5). The PIRI spectrum of the $\tilde{B}^+$ state acquired via the 6b vibration of the ground cationic state has also been assigned assuming an allowed $\tilde{B}^+\leftarrow\tilde{X}^+$ transition, with the most intense peak observed being the $6b^1_1$ transition with a 6a progression built on it. The structure observed to the left of it at 18 241 cm^{-1} can be satisfactorily assigned as $6b^0_1 16b^1_0 18b^1_0$, with a 6a progression built on it.

Other assignment of the vibrations observed in the PIRI spectra of $\tilde{B}^+$ state followed the values obtained for the ground cationic state, assuming that the energy values do not change much in the $^2B_1$ excited state. The peak at 18 219 cm^{-1} in the PIRI spectrum via the origin of the $\tilde{X}^+$ state is confidently assigned as the origin of the $\tilde{B}^+$ state and the rest of the spectrum is assigned accordingly, as shown in Figure 1 and tabulated in Table 3. Assignments of the PIRI spectra via the 16a16b and 6b vibrations of the $\tilde{X}^+$ state are provided in Table 4a and b. The assignments of the vibrational features of the acquired REMPD spectra are tabulated in Table 5 and shown in Figure 3.

Vibrational features scanned in the PIRI/REMPD spectra are primarily of a_1 symmetry (z-polarized), though some vibrational features of b_2 and b_1 symmetry appear. Many of the present assignments are the same as those of Ripoche et al.[16] if one simply deletes a 16a vibration from the attribution.

TABLE 4: Assignments for the PIRI Spectrum of the $\tilde{B}^+$ State of the Chlorobenzene Cation via the 16a16b and 6b Vibrations of the Ground Ionic State and the Energy Values of the Vibrations

frequency (cm^{-1})	proposed assignment	distance from the first peak (cm^{-1})
	16a16b vibration	
17 924	$16a^1_1 16b^1_1$	0
18 150	$16a^1_0 16b^2_1$	226
18 306	$16a^1_1 16b^1_1 6a^1_0$	382
18 467	$16a^1_1 16b^1_1 6b^1_0$	543
18 524	$16a^1_1 16b^2_1 6a^1_0$	600
18 559	$16a^1_1 16b^1_1 12^1_0$	635
18 654	$16a^1_1 16b^1_1 5^1_0$	730
18 686	$16a^1_1 16b^1_1 6a^2_0$	762
	6b vibration	
18 241	$6b^0_1 16b^1_0 18b^1_0$	0
18 255	$6b^1_1$	14
18 625	$6b^0_1 16b^1_0 18b^1_0 6a^1_0$	384
18 639	$6b^1_1 6a^1_0$	398

TABLE 5: Proposed Assignments of the REMPD Spectra and the Energy Values of the Vibrations

frequency (cm^{-1})	proposed assignments	distance from origin (cm^{-1})
17 765	$6a^1_2$	453
17 800	$6a^0_1$	418
18 049	11^0_1	167
18 129		89
18 147	$6a^2_2$	71
18 188	$6a^1_1$	30
18 218	0^0_0	0
18 568	$6a^2_1$	348
18 603	$6a^1_0$	383
18 757		537
18 783	$6b^1_0$	565
18 817		601
18 930	$6a^1_0 18b^1_0$	712
18 983	$6a^2_0$	764
19 043	$6a^1_0 16b^1_0 16a^1_0$	826
19 085	$18a^1_0$	865
19 114	$6b^1_0 18b^1_0$	894
19 152	$6b^1_0 6a^1_0$	931
19 228	1^1_0	1009
19 352	$7a^1_0$	1133
19 367	$6a^3_0$	1149
19 427	$6a^2_0 16b^1_0 16a^1_0$	1213
19 453		1237
19 476	$18a^1_0 6a^1_0$	1257
19 494	$9a^1_0$	1278
19 540	$6b^1_0 6a^2_0$	1324
19 604	$1^1_0 6a^1_0$	1388
19 653		1434
19 683		1465
19 706	$19a^1_0$	1487
19 747	$6a^4_0$	1532
19 853	$18a^1_0 6a^2_0$	1635
19 890		1673
19 920		1701
19 943		1725
19 973	$18a^2_0$	1754
20 007		1790
20 040		1823
20 086		1869
20 157	$6a^5_0$	1942
20 199		1983
20 226	$18a^1_0 6a^3_0$	2005

Conclusion

The cold PIRI spectra of the chlorobenzene cation via the origin and 16a16b and 6b vibrational levels of the ground ionic state throw a different light on the ordering of the energy levels of the excited electronic states. In the PIRI spectrum of the chlorobenzene cation, as found for fluorobenzene, the transition takes place from the ground state ($\tilde{X}^+$ state with $^2B_1$ symmetry) to an excited state of the cation with $^2B_1$ symmetry, thus giving rise to the observance of the origin of the excited ionic state at

18 219 cm^{-1}. The observed vibrational structure has been adequately assigned using the calculated and experimental vibrational frequencies of the cation ground state. The value obtained for the origin of the $\tilde{B}^+$ state (from the ground neutral state) in the PIRI spectra corresponds to approximately the same value of 11.32 eV obtained in PES by Potts et al.,[7] Kimura et al.,[7] and by Ruščič et al.[7]

Acknowledgment. This work was supported by a grant from the U.S. Department of Energy, Division of Chemical Sciences. Dr. C. Cossart-Magos thanks Dr. I. Dimicoli for many stimulating discussions.

References and Notes

(1) (a) Taylor, D. P.; Goode, J. G.; LeClaire, J. E.; Johnson, P. M. *J. Chem. Phys*. **1995**, *103*, 6293. (b) Goode, J. G.; LeClaire, J. E.; Johnson, P. M. *Int. J. Mass. Spectrom. Ion. Processes* **1996**, *159*, 49.

(2) Goode, J. G.; Hofstein, J. D.; Johnson, P. M. *J. Chem. Phys.* **1997**, *107*, 1703.

(3) LeClaire, J. E.; Anand, R.; Johnson, P. M. *J. Chem. Phys.* **1997**, *106*, 6785.

(4) Anand, R.; LeClaire, J. E.; Johnson, P. M. *J. Phys. Chem. A.* **1999**, *103*, 2618.

(5) (a) Zhu, L.; Johnson, P. M. *J. Chem. Phys.* **1991**, *94*, 5769. (b) Johnson, P. M.; Zhu, L. *Int. J. Mass. Spectrom. Ion. Processes* **1991**, *131*, 193.

(6) Streets, D. G.; Ceasar, G. P. *Mol. Phys.* **1973**, *26*, 1037.

(7) (a) Kimura, K.; Katsumata, S.; Achiba, Y.; Yamazaki, T.; Iwata, S. *Handbook of He (I) Photoelectron Spectra of Fundamental Organic Molecules*; Halsted: New York, 1981. (b) Ruščič, B.; Klasinc, L.; Wolf, A.; Knop, J. V. *J. Phys. Chem.* **1981**, *85*, 1486. (c) Potts, A. W.; Lyus, M. L.; Lee, E. P. F.; Fattahallah, G. H. *J. Chem. Soc., Faraday Trans. 2* **1980**, *76*, 556.

(8) Fujisawa, S.; Ohno, K.; Masuda, S.; Harada, Y. *J. Am. Chem. Soc.* **1986**, *108*, 6505.

(9) Maier, J. P.; Marthaler, O. *Chem. Phys.* **1978**, *32*, 419.

(10) Leismann, H.; Scharf, H.-D.; Strassburger, W.; Wollmer A. *J. Photochem.* **1983**, *21*, 275.

(11) (a) Anderson, S. L.; Rider, D. M.; Zare, R. N. *Chem. Phys. Lett.* **1982**, *93*, 11. (b) Asselin, P.; Piuzzi, F.; Le Calvé, J.; Mons, M.; Dimicoli, I. *Chem. Phys.* **1994**, *181*, 271. (c) Asselin, P.; Gouzerh, A.; Piuzzi, F.; Dimicoli, I. *Chem. Phys.* **1993**, *175*, 387.

(12) Wright, T. G.; Panov, S. I.; Miller, T. A. *J. Chem. Phys*. **1995**, *102*, 4793.

(13) Lembach, G.; Brutschy, B. *Chem. Phys. Lett.* **1997**, *273*, 421.

(14) Woodward, A. M.; Chupka, W. A.; Colson, S. D. *J. Phys. Chem.* **1984**, *88*, 4567.

(15) Boesl, U. *J. Phys. Chem.* **1991**, *95*, 2949.

(16) Ripoche, X.; Dimicoli, I.; Le Calvé, J.; Piuzzi, F.; Botter, R. *Chem. Phys.* **1988**, *124*, 305.

(17) Friedman, R. S., Kelsall, B. J.; Andrews, L. *J. Phys. Chem.* **1984**, *88*, 1944.

(18) Frisch, M. J.; Trucks, G. W.; Schlegel, H. B.; Gill, P. M. W.; Johnson, B. G.; Robb, M. A.; Cheeseman, J. R.; Keith, T. A.; Petersson, G. A.; Montgomery, J. A.; Raghavachari, K.; Al-Laham, M. A.; Zakrzewski, V. G.; Ortiz, J. V.; Foresman, J. B.; Cioslowski, J.; Stefanov, B. B.; Nanayakkara, A.; Challacombe, M.; Peng, C. Y.; Ayala, P. Y.; Chen, W.; Wong, M. W.; Andres, J. L.; Relpogle, E. S.; Gomperts, R.; Martin, R. L.; Fox, D. J.; Binkley, J. S.; Defrees, D. J.; Baker, J.; Stewart, J. P.; Head-Gordon, M.; Gonzalez, C.; Pople, J. A. *Gaussian 94 (Revision A.1)*, Gaussian, Inc.: Pittsburgh, PA, 1995.

(19) Dupuis, M.; Spangler, D.; Wendoloski, J. J. *Gamess (QG01)*. National Resource for Computations in Chemistry Software Catalog, University of California: Berkeley, CA, 1980.